Carbohydrate Polymers 117 (2015) 910–916

Contents lists available at ScienceDirect

Carbohydrate Polymers

journal homepage: www.elsevier.com/locate/carbpol

Trapping by amylose of the aliphatic chain grafted onto chlorogenic acid: Importance of the graft position

P. Le-Bail[a,*], C. Lorentz[b], G. Pencreac'h[b], S. Soultani-Vigneron[b], B. Pontoire[a], L.J. López Giraldo[c], P. Villeneuve[c], J. Hendrickx[d], V. Tran[d]

[a] INRA, UR 1268, Biopolymères Interactions Assemblages, Rue de la Géraudière, BP 71627, F-44316 Nantes Cedex 3, France
[b] "Mer, Molécules, Santé" (MMS), EA 2160 IUT de Laval,Département Génie Biologique, 52 rue des Docteurs Calmette et Guérin, BP 2045, F-53020 Laval Cedex 09, France
[c] UMR 1208 INRA, CIRAD, Montpellier SupAgro, Université Montpellier 2, 2 Place Viala, 34060 Montpellier Cedex 2, France
[d] UMR-CNRS no. 6286 Biotechnologie, Biocatalyse & Biorégulation (U3B), 2, rue de la Houssinière, BP 92208, 44322 Nantes Cedex 3, France

ARTICLE INFO

Article history:
Received 25 April 2014
Received in revised form
16 September 2014
Accepted 2 October 2014
Available online 23 October 2014

Keywords:
Amylose complex
Palmitoyl chlorogenic acid
CP/MAS NMR
DSC
X-ray diffraction
Molecular modeling

ABSTRACT

5-Caffeoylquinic acid (chlorogenic acid), is classified in acid–phenols family and as polyphenolic compounds it possesses antioxidant activity. The oxydative modification of chlorogenic acid in foods may lead to alteration of their qualities; to counteract these degradation effects, molecular encapsulation was used to protect chlorogenic acid. Amylose can interact strongly with a number of small molecules, including lipids. In order to enable chlorogenic acid complexation by amylose, a C16 aliphatic chain was previously grafted onto the cycle of quinic acid. This work showed that for the two lipophilic derivatives of chlorogenic acid: hexadecyl chlorogenate obtained by alkylation and 3-*O*-palmitoyl chlorogenic acid obtained by acylation; only the 3-*O*-palmitoyl chlorogenic acid complexed amylose. The chlorogenic acid derivatives were studied by X-ray diffraction, differential scanning calorimetry and NMR to elucidate the interaction. By comparing the results with previous work on the complexation of amylose by 4-*O*-palmitoyl chlorogenic acid, the importance of the aliphatic chain position on the cycle of the quinic acid is clearly highlighted. A study in molecular modeling helped to understand the difference in behavior relative to amylose of these three derivatives of chlorogenic acid.

1. Introduction

Oxidation is probably one of the major parameters causing spoilage of food products. Oxidative damage affects the nutritional and sensory qualities of products and can have repercussions on the health of consumers. In this context, various preventive means are available to limit these phenomena. Among them, the valorization of antioxidants of plant origin for food is a major challenge for research and industry. Among natural antioxidants, phenolic compounds, particularly phenolic acids, have aroused increasing interest (Sun-Waterhouse, 2011). Phenolic acids include chlorogenic acids, which are esters of caffeic acid and quinic acid. 5-caffeoylquinic acid (chlorogenic acid) is one of the major polyphenol compounds found in numerous plant species (Clifford, 1999) and possesses antioxidant properties (Kono et al., 1997; Zang, Cosma, Gardner, Castranova, & Vallyathan, 2003). The addition of these polar molecules to the formulation of emulsions is delicate (as they are fragile and easily oxidized molecules) and may not only be accompanied by a decrease in their effectiveness in protecting against lipid oxidation, but also contribute to a loss of their nutritional intake. The first free radicals are often produced in the aqueous phase, as this is the environment through which oxygen diffuses from the outside. However, this aqueous phase can also provide opportunities for protecting these molecules of interest *via* assemblies with biopolymers such as starch.

Autoxidation of chlorogenic acid, which occurs during food processing for example, may lead to the formation of brown polymerized products (Ingraham & Corse, 1951). To overcome these drawbacks, several encapsulation and microencapsulation methods have been described to protect and improve chlorogenic acid stability (Shi et al., 2007; Zhao, Wang, Yang, & Tao, 2010). However, molecular encapsulation with amylose, the linear component of starch, has little been reported, although it is known from the literature that the use of amylose to form an inclusion complex can provide very interesting applications to protect bioactive molecules. Indeed, it is well established that amylose can form

* Corresponding author. Tel.: +33 240675054; fax: +33 240675084.
E-mail address: patricia.le-bail@nantes.inra.fr (P. Le-Bail).

http://dx.doi.org/10.1016/j.carbpol.2014.10.029
0144-8617/

helical inclusion complexes with a variety of compounds such as alcohols (Brisson, Chanzy, & Winter, 1991; Buléon, Delage, Brisson, & Chanzy, 1990; Rappenecker & Zugenmaier, 1981), and aroma compounds (Biais, Le Bail, Robert, Pontoire, & Buleon, 2006; Nuessli, Sigg, Conde-Petit, & Escher, 1997) in aqueous solution. The molecular organization of amylose complexes with various fatty acids has been extensively studied (Biliaderis, & Galloway, 1989; Biliaderis, Page, Slade, & Sirett, 1985; Godet, Bizot, & Buléon, 1995; Godet, Buléon, Tran, & Colonna, 1993), and a model involving inclusion of the aliphatic part of the lipid in the cavity of amylose is commonly accepted (Godet, Tran, Colonna, Buléon, & Pezolet, 1995). However Lorentz et al. (2012) studied the complexation of amylose with a derivative of chlorogenic acid. These authors reported that 4-*O* palmitoyl chlorogenic acid complexed amylose by trapping the grafted aliphatic chain in the helical cavity of amylose, thereby protecting the molecule against oxidation.

The strategy of this study was to reduce the polarity of the molecules significantly by grafting aliphatic chains onto several sites of the quinic ring in order to adjust their position in food matrices. A 16-carbon-long aliphatic chain was first grafted onto chlorogenic acid by a lipase-catalyzed synthesis (Lorentz et al., 2010) in order to obtain a chlorogenic acid derivative (3-*O* palmitoyl chlorogenic acid Fig. 1(2)). On the other hand, a chemical synthesis (Chebil, Humeau, Falcimaigne, Engasser, & Ghoul, 2006; Figueroa-Espinoza & Villeneuve, 2005; Villeneuve, 2007) provided a second chlorogenic acid derivative, hexadecyl chlorogenate, Fig. 1(1). Then, the ability of amylose to trap the carbon chain was studied by X-ray diffraction, differential scanning calorimetry and solid state nuclear magnetic resonance and the results were compared to the study of Lorentz and collaborators. The importance of the graft position on the ring of quinic acid was also investigated by molecular modeling.

2. Materials and methods

2.1. Biological and chemical materials

The lipase used was Novozym 435® purchased from Novozymes (Dk). It consisted of lipase B from *Candida antarctica* (lipase B) immobilized on acrylic resin. All solvents and reagents used were obtained from commercial sources and were of either HPLC or analytical grade. Palmitic acid and silica gel plates were purchased from Sigma-Aldrich, France. Chlorogenic acid was purchased from Acros, France, and was 99% pure. Potato amylose (type III), essentially free of amylopectin, was obtained from Sigma-Aldrich (France) and used as received.

2.2. Lipase-catalyzed synthesis of 3-O-palmitoyl chlorogenic acid

3-*O* palmitoyl chlorogenic acid is one of the two products (3-*O*-palmitoyl chlorogenic acid and 4-*O*-palmitoyl chlorogenic acid) from the Novozym 453-catalyzed esterification of chlorogenic acid with palmitic acid. Their synthesis and purification were performed as previously described (Lorentz et al., 2010). Briefly, chlorogenic acid, palmitic acid and Novozym 435 were dried for two days over P_2O_5 before use. In these conditions, the initial water activity (a_w) of the reaction medium, determined using an AqualabLite® (Decagon Devices Inc., USA), was below 0.2. The reaction was carried out in 2-mL Eppendorf tubes in the dark. The reaction mixture consisted of 28 μmol of chlorogenic acid and 1.12 mmol of palmitic acid (substrate ratio of 40) in 1 mL of 2-methyl–2-butanol (2M2B). Palmitic acid and chlorogenic acid were first solubilized for 12 h in 2M2B under stirring at 1000 rpm and at 60 °C in an Eppendorf Thermomixer (Roucaire, France). Then, 200 mg of molecular sieves (3 Å), previously dried overnight at 200 °C, was added and the reaction was initiated by addition of 40 mg of enzyme.

After 7 days of reaction, the immobilized enzyme and molecular sieves were filtered off (0.22 μm), the solvent was evaporated under vacuum and 3-*O*-palmitoyl chlorogenic acid and 4-*O*-palmitoyl chlorogenic acid were isolated by Sephadex LH-20 chromatography using chloroform/methanol (70/30, v/v) as the eluent. Purification was completed by means of preparative TLC. As determined by HPLC, the final product was at least 98% pure.

2.3. Chemical synthesis of hexadecyl chlorogenate

In a 500-mL glass vessel, 10 mmol of 5-CQA was diluted in 240 mL of methanol. Amberlite IR120 H (10 g), previously dried at 110 °C for 48 h, was added to the reaction mixture, which was then stirred in an orbital shaker (250 rpm) for 9 h at 55 °C. After cooling to room temperature, the reaction medium was filtered on a 1.6-μm glass microfiber filter (Whatman International Ltd., Maidstone, England). Methanol was then evaporated under vacuum. Chloroform (150 mL) was added, and the solution was dried over sodium sulfate, filtered on a 1.6-μm glass microfiber filter and evaporated under vacuum at 50 °C. The powder obtained was identified by mass spectrometry.

2.4. Preparation of amylose complexes

The complexation experiments were conducted using chlorogenic acid and its derivatives: 3-*O*-palmitoyl chlorogenic acid and hexadecyl chlorogenate. Before heating and mixing amylose and chlorogenic acid derivatives, a nitrogen flow was first passed through the samples for 15 min to prevent their oxidation during heating.

Amylose was dispersed in pure water 1% (w/v) (200 mg/20 mL) at 145 °C for 45 min in a glass tube with a screw cap. As the solubility in water of the chlorogenic acid derivatives used is very low at room temperature, 10 mg of chlorogenic acid derivatives was solubilized and preheated in 5 mL of water at 90 °C and added to amylose solution after its cooling at 90 °C. The mixture was then maintained at 90 °C for 10 min, cooled to room temperature and stored for 48 h. Next, the precipitate was collected by centrifugation (2000 × *g* for 10 min) and the water content adjusted by desorption at $a_w = 0.75$ over saturated NaCl solution before X-ray, DSC and solid state NMR analyses. Amylose solution was prepared in the same conditions and used as the reference.

All samples were prepared in triplicate and each measurement was made three times.

2.5. Differential scanning calorimetry

DSC thermograms were recorded using an automated heat flux differential scanning calorimeter (TA Instruments, Q100). Stainless steel high pressure cells (TA Instruments, ref: 900825.902) were used. The system was calibrated with indium and a pan containing 12 μL of water was taken as the reference. Eight milligrams of sample was weighed into pans and 12 μL of water was added. Two successive scans were run in triplicate at 3 °C/min from 1 °C to 140 °C for the first scan and from 1 °C to 160 °C at 1 °C/min for the second, separated by a cooling stage at 3 °C/min.

2.6. X-ray diffraction

Fifty milligrams of sample, equilibrated at $a_w = 0.75$, was sealed in a copper ring between two adhesive tape sheets to prevent any change in water content. The sample was examined by Wide Angle X-ray Scattering. Measurements were performed using a D8 Discover spectrometer from Bruker-AXS. Cu $K\alpha_1$ radiation (Cu $K\alpha_1 = 1.5405$ Å), produced in a sealed tube at 40 kV and 40 mA, was selected and parallelized using a double Gobël mirror parallel optics

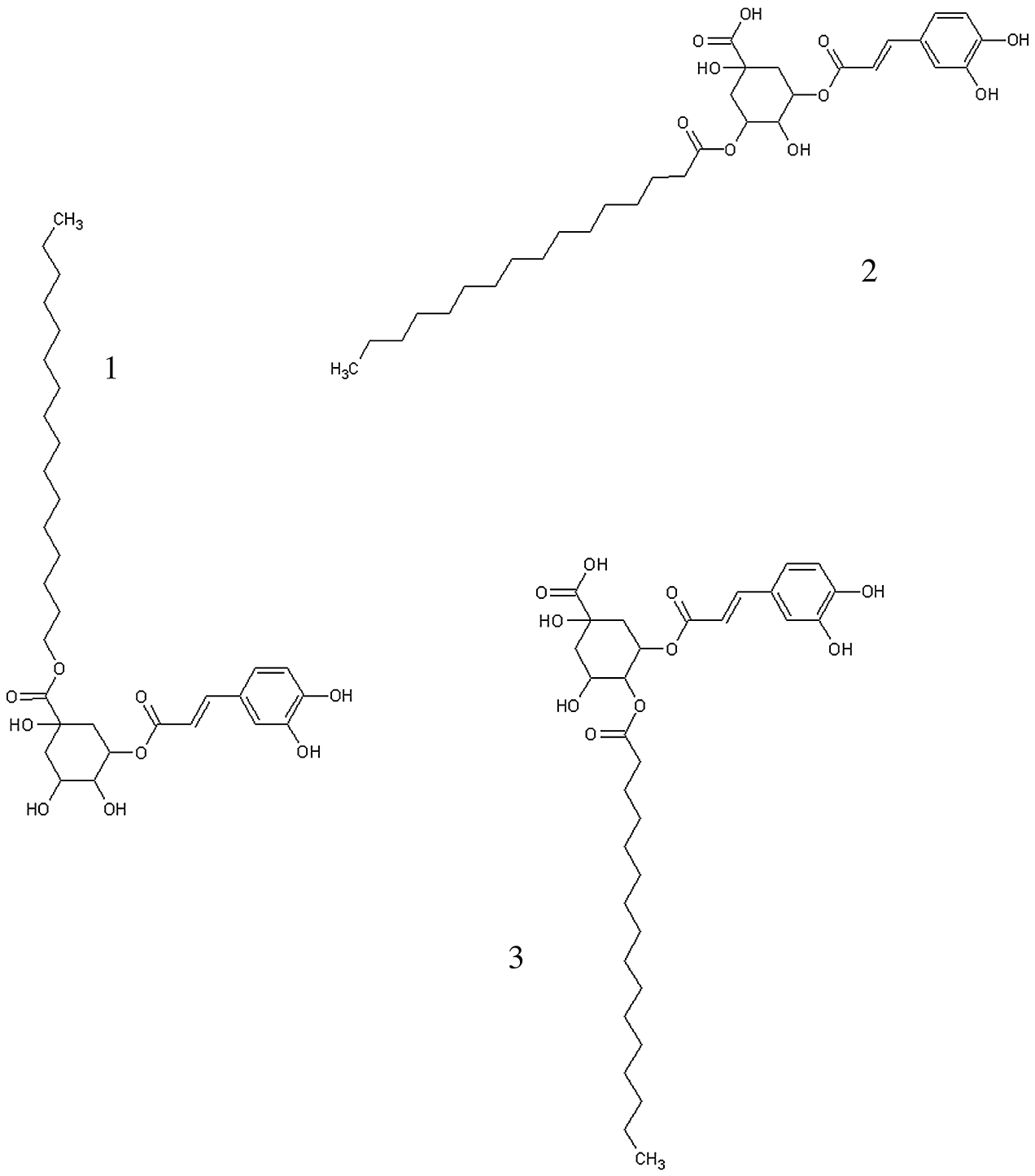

Fig. 1. Chemical structure of (1) hexadecyl chlorogenate; (2) 3-*O*-palmitoyl chlorogenic acid and (3) 4-*O*-palmitoyl chlorogenic acid.

system and collimated to produce a 500-μm beam diameter and sample alignment by microscopic video and laser. Data were monitored by a GADDS 2D detector for 10 min and normalized between 3 and 30° (2θ).

2.7. ^{13}C solid state NMR

NMR experiments were performed on a Bruker DMX-400 spectrometer operating at a ^{13}C frequency of 100.62 MHz and equipped with a double resonance H/X CP/MAS 4 mm probe. The MAS rate was fixed at 5000 Hz and each experiment was recorded at ambient temperature (294 ± 1 K). The Cross Polarization pulse sequence used a 3.75 μs 90° proton pulse, a 1 ms contact time at 66.7 kHz and a 10 s recycle time for an acquisition time of 17 ms during which dipolar decoupling was applied. Typically, 5120 scans were acquired for each spectrum. Chemical shifts were calibrated with external glycine, assigning the carbonyl carbon at 176.03 ppm.

2.8. Molecular modeling

Experimental research of the 3D structures of the relevant derivatives of quinic acid was made in the Protein Data Bank, PDB

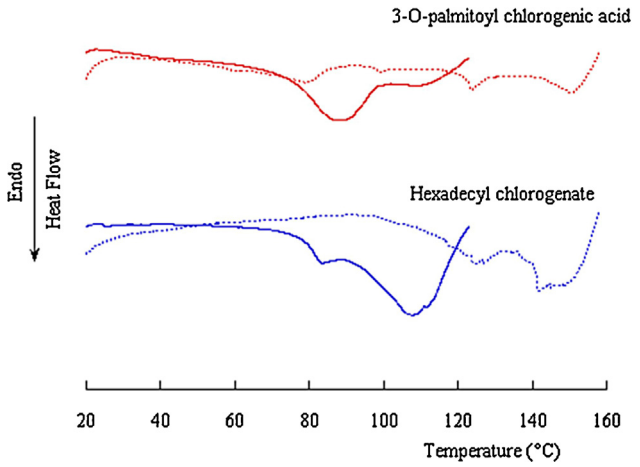

Fig. 2. DSC thermograms of amylose–hexadecyl chlorogenate and amylose–3-*O*-palmitoyl chlorogenic acid.

(http://www.pdb.org/) and the Cambridge Structural Database, CSD (http://www.ccdc.cam.ac.uk/). The energetic calculations were performed in Discovery Studio 2.0 (ACCELRYS) (Accelrys Software Inc., Discovery Studio Modeling Environment, San Diego, USA) with the CHARMm force field (Chemistry at HARvard Macromolecular Mechanics) sufficiently robust and suitable for small molecules. All the energetic minimizations of molecular structures were made with the same protocol: relaxation in a vacuum without geometric constraints with the 'steepest descent' algorithm and with a stopping criterion of one convergence gradient (grms) = 0.01 A. The molecular representations were made with the software PYMOL (The PyMOL Molecular Graphics System, Version 1.5.0.4 Schrödinger, LLC).

2.9. Statistical analysis

Statistical analysis was performed on the basis of results obtained in triplicate. The average and standard deviation were calculated for each experiment.

3. Results and discussion

3.1. Thermal analysis

In the present experiment, the complexing abilities of amylose with hexadecyl chlorogenate and 3-*O*-palmitoyl chlorogenic acid were determined by differential scanning calorimetry and compared to the reference (amylose without ligand) and to the results obtained with chlorogenic acid and 4-*O*-palmitoyl chlorogenic acid in the previous publication (Lorentz et al., 2012).

A differential scanning calorimetry study (data not shown) was also conducted for pure ligands in excess water. One endotherm was observed at $65 \pm 2\,^{\circ}C$ (chlorogenic acid), $51 \pm 2\,^{\circ}C$ (4-*O*-palmitoyl chlorogenic acid), $91 \pm 2\,^{\circ}C$ (3-*O*-palmitoyl chlorogenic acid), and $84 \pm 2\,^{\circ}C$ (hexadecyl chlorogenate).

The thermograms recorded are shown in Fig. 2. The second scan was used to prove reorganization during the cooling carried out between the two heating scans and, especially, the well-known melting/recrystallization reversibility of amylose lipid complexes (Biliaderis & Galloway, 1989).

Thermogram obtained from amylose–hexadecyl chlorogenate assembly presents a similar behavior to the thermograms obtained from the reference (amylose without ligand) and from the amylose–chlorogenic acid assembly (Lorentz et al., 2012), with a broad endotherm at $107 \pm 2\,^{\circ}C$ during the first heating. This was interpreted by these authors as a partial dispersion of amylose at $145 \pm 2\,^{\circ}C$, only one part of amylose would be dispersed causing a fast retrogradation during cooling and storage. On the second scan, both endotherms are detected at around $120 \pm 2\,^{\circ}C$ and $150 \pm 3\,^{\circ}C$, and have been attributed by these same authors to retrograded amylose with poor crystallinity obtained during the cooling between the two heating scans and to the initial amylose possessing a good crystalline organization, respectively. The thermogram of amylose–hexadecyl chlorogenate also presents an endotherm at $83 \pm 2\,^{\circ}C$, noticeable only on the first scan. This peak was attributed to the melting of hexadecyl chlorogenate.

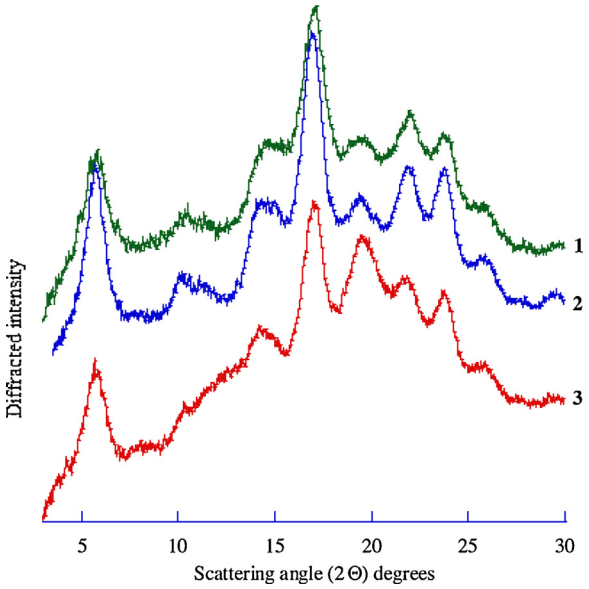

Fig. 3. X-ray diffraction spectra of 1: amylose without ligand; 2: amylose complexed with hexadecyl chlorogenate and 3: amylose complexed with 3-*O*-palmitoyl chlorogenic acid.

Thermogram of amylose–3-*O*-palmitoyl chlorogenic acid complex (Fig. 2) presents one more endotherm, obvious on the first and second scans and highlighting the presence of complexes. Nevertheless, the endotherm on the first scan was at $88 \pm 2\,^{\circ}C$ and at $80 \pm 2\,^{\circ}C$ on the second scan. The higher temperature value for endotherm on the first scan can be explained by the superimposition of the complex melting endotherm at $80\,^{\circ}C$ and the 3-*O*-palmitoyl chlorogenic acid melting endotherm at $91\,^{\circ}C$.

However, the low melting temperature of the complexes ($80 \pm 2\,^{\circ}C$), also observed for the complex amylose–4-*O*-palmitoyl chlorogenic acid (Lorentz et al., 2012), reflects a very poor crystalline organization (Biliaderis & Galloway, 1989).

Based on our results, it can be concluded that hexadecyl chlorogenate do not induce interaction with amylose. However, complexation of 3-*O*-palmitoyl chlorogenic acid with amylose was highlighted and the observed low melting temperature of the complexes could result from a poorly ordered or amorphous complex.

3.2. X-ray diffraction study

Fig. 3 displays the X-ray diffraction diagrams of (1) amylose without ligand; (2) amylose complexed with hexadecyl chlorogenate and (3) amylose complexed with 3-*O*-palmitoyl chlorogenic acid.

All X-ray diagrams obtained display the typical B-type crystallinity patterns ($2\Theta = 5.6^{\circ}$, 10.1°, 11.3°, 14.9°, 17°, 19.5°, 22°, 23.9°) due to the presence of retrograded amylose. The results are identical to those establishes for the amylose complexed with

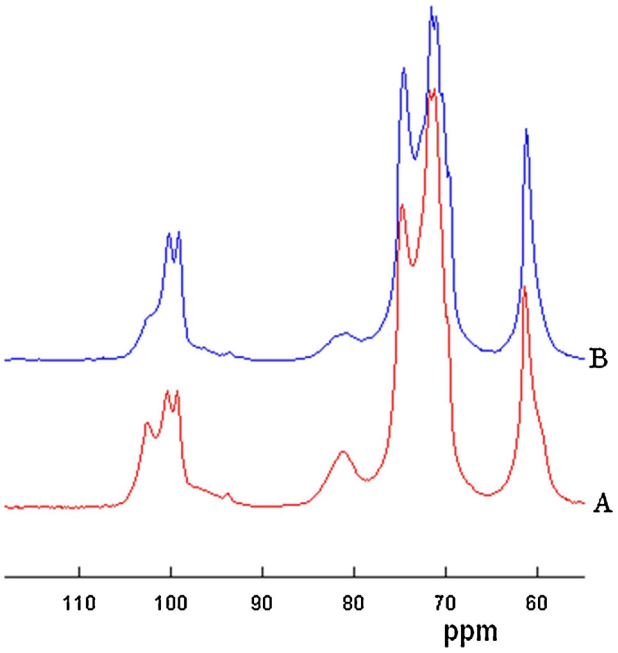

Fig. 4. ^{13}C CP/MAS NMR spectra of (A) amylose complexed with 3-*O*-palmitoyl chlorogenic acid and (B) amylose complexed with hexadecyl chlorogenate.

chlorogenic acid and 4-*O*-palmitoyl chlorogenic acid (Lorentz et al., 2012).

However, like observed Lorentz et al. (2012), the strong diffusion bump centered at 19° (2Θ) for amylose–3-*O*-palmitoyl assemblies, and the shift of the peak at 19.5° (19.8°) and the increase in its intensity suggest the formation of a V-type amorphous compound.

3.3. ^{13}C solid state NMR

Solid state NMR has proved to be a powerful tool for characterizing some degrees of molecular order, such as helicity, in the structure of starchy substrates (Gidley & Bociek, 1985; Horii, Yamamoto, Hirai, & Kitamaru, 1987; Paris, Bizot, Emery, Buzaré, & Buleon, 1999; Singh, Ali, & Divakar, 1993; Veregin, Fyfe, Marchessault, & Taylor, 1986).

Spectrum of the amylose–hexadecyl chlorogenate (Fig. 4B) is close to the amylose without ligand and to the amylose–chlorogenic acid spectra (Lorentz et al., 2012), with a doublet at 100.5 and 99.3 ppm, namely to the B-type spectrum (Gidley & Bociek, 1988; Veregin, Fyfe, Marchessault, & Taylor, 1987a). According to Paris et al. (Paris, Bizot, Emery, Buzaré, & Buléon, 2001), the shoulder present on the C1 doublet detected in the spectrum of the amylose–chlorogenic acid complex may be attributed to the amorphous background.

Like the spectrum of the amylose–4-*O*-palmitoyl chlorogenic acid complex (Lorentz et al., 2012), the amylose–3-*O*-palmitoyl chlorogenic acid complex spectrum (Fig. 4A) displays the resonances of B-type amylose in addition to signals typical of a V-type structure (Gidley & Bociek, 1985; Le Bail, Rondeau & Buléon, 2005). Peaks observed at 102.7, 81.4, 74.9, 71.6, 61.3 and 60 ppm were assigned to C1, C4, C3, C2—C5, and C6 carbons, respectively, and are characteristic of the V_{6I} form (Gidley & Bociek, 1985; Le Bail et al., 2005). The doublet signal in the C1-region at 100.5 and 99.3 ppm was also observed and indicated the presence of double helices due to non-complexed B-type amylose (Gidley & Bociek, 1988; Veregin, Fyfe, Marchessault, & Taylor, 1987b).

The characteristic peak of the typical V conformation (102.7 ppm) presents an intensity significantly lower for the amylose–3-*O*-palmitoyl chlorogenic acid complex than for the amylose–4-*O*-palmitoyl chlorogenic acid complex shown in the previous publication (Lorentz et al., 2012), showing a poorer interaction between 3-*O*-palmitoyl chlorogenic acid and amylose than between 4-*O*-palmitoyl chlorogenic acid and amylose.

These results agreed with the calorimetry study, showing interactions between 3-*O*-palmitoyl chlorogenic acid and amylose, while chemical shifts observed for the carbon signals in the spectrum, especially C1, were clearly assigned to the spectrum of the V_{6I} form (Le Bail et al., 2005). This confirms that, like for the amylose complex obtained with 4-*O*-palmitoyl chlorogenic acid, only the graft was included inside the helical cavity of amylose.

3.4. Molecular modeling study

A molecular modeling study was conducted for hexadecyl chlorogenate, 3-*O*-palmitoyl chlorogenic acid, and 4-*O*-palmitoyl chlorogenic acid to understand the importance of the graft position on the ring of quinic acid. Chlorogenic acid is an ester of caffeic acid and quinic acid, namely 5-caffeoylquinic acid, classed as an amino-phenol. Quinic acid is a chiral reagent and its other name is (1S, 3R, 4S, 5R)—1,3,4,5-tetrahydroxycyclohexanecarboxylic acid.

3.4.1. Quinic acid conformation

A first comprehensive research of the quinic and caffeic acid derivatives and the complexes of these molecules with proteins was made in the PDB and the CSD. In the PDB, only the complexes for which the involved substrates did not have double bonds in the six-membered ring, or starting from this ring, were selected. Otherwise, the substitutions in positions 3 and 5 comply with the R configuration of these asymmetric carbon atoms. Three structures match these criteria (PDB codes: 3JYP, 4IUO, 4GUI). For the CSD, the derivatives forming a bicyclic structure preventing the interconversion 'chair' of the quinic acid ring were also excluded. Another structure of quinic acid is reported (CSD code: VUXRIP). Furthermore, the crystallographic structure of chlorogenic acid is available (code CDS: DIJWAU) (Martin, Lilley, Fasshaw, Begley, & Magnolato, 1987).

All these structures are superimposable on the basis of the quinic acid ring and they adopt the $_1C^4$ 'chair' conformation, by analogy with the terminology of glucopyranose rings. This means that, compared to the average plane of the ring (as shown in Fig. 5), the carbon atoms C1 and C4 are below and above the mean plane, respectively.

3.4.2. Chlorogenic acid conformation

The carboxylic acid group carried on C1 is in the equatorial position as is the *O*-caffeoyl group carried on C5. The hydroxyl groups carried on C3 and C4 are in axial and equatorial positions, respectively.

The experimental geometry of chlorogenic acid found in the CSD therefore seemed suitable for grafting palmitic acid in position 1 (carboxylic acid group) and in positions 3 and 4 (hydroxyl groups). To explain the experimental results, we focused on the possible conformations of the derivative grafted in the C1 position.

3.4.3. Conformation of the derivative grafted in the C1 position

In addition to the intrinsic flexibility of the aliphatic chain, the following degrees of freedom were taken into account in an analysis of possible conformations: rotations around single bonds (shown in Fig. 6) which were sampled according to their contexts.

A first series of calculations starting from the $_1C^4$ 'chair' form was performed. In all these calculations, the equatorial, and almost opposite, directions of the substituents in positions 1 and 5 did not allow them to be closer, thus providing an explanation for the impossibility of forming a complex with the amylose chain.

A new series of calculations was made from a reconstructed geometry *in silico* of quinic acid in the other $_4C^1$ 'chair' conformation

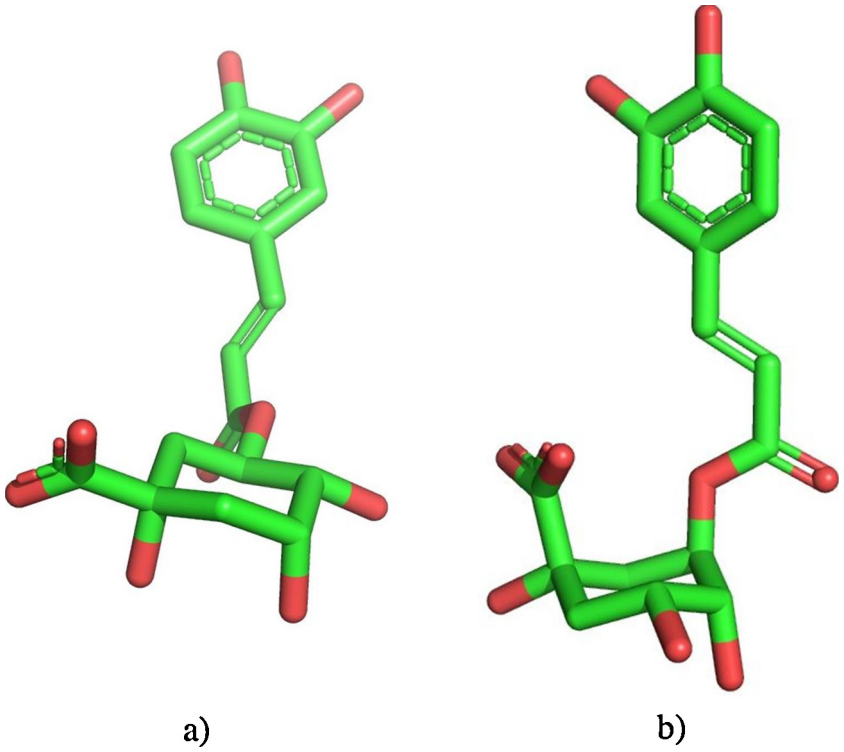

Fig. 5. Chlorogenic acid conformations by molecular modeling. (a) $_1C^4$ conformation and (b) $_4C^1$ conformation.

where the substituents attached to C1 and C5 are in axial positions. The same protocol for taking into account the degrees of freedom described above was used.

The best solutions are analyzed as follows:

For chlorogenic acid, the energy calculations show a difference of 3.2 kcal/mol in favor of the $_1C^4$ 'chair' conformation. This is consistent with experimental results where the only crystalline forms found for quinic and chlorogenic acids are in the $_1C^4$ form. In contrast, for the hexadecyl derivatives grafted in the C1 position, the $_4C^1$ form is clearly favored over $_1C^4$ with a difference of 12.4 kcal mol (Fig. 7(a) $_4C^1$ and (b) $_1C^4$).

The energy difference of 12.4 kcal/mol is mainly due to hydrophobic interactions between the aromatic ring and the aliphatic chain, which may be closer because of the axial orientations of the substituents attached in the C1 and C5 positions. This energy difference may explain the tilting of the $_1C^4$ form into the $_4C^1$ form, and thus the aliphatic chain cannot be complexed by the amylose chain unlike in the other conformations.

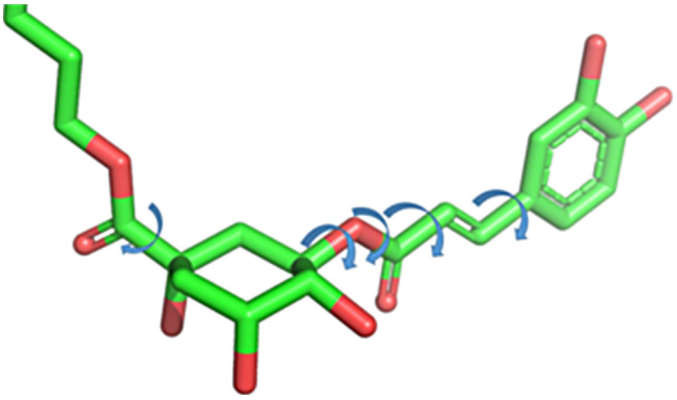

Fig. 6. The rotations around single bonds of chlorogenic acid taken into account to determine different conformations of hexadecyl chlorogenate by molecular modeling.

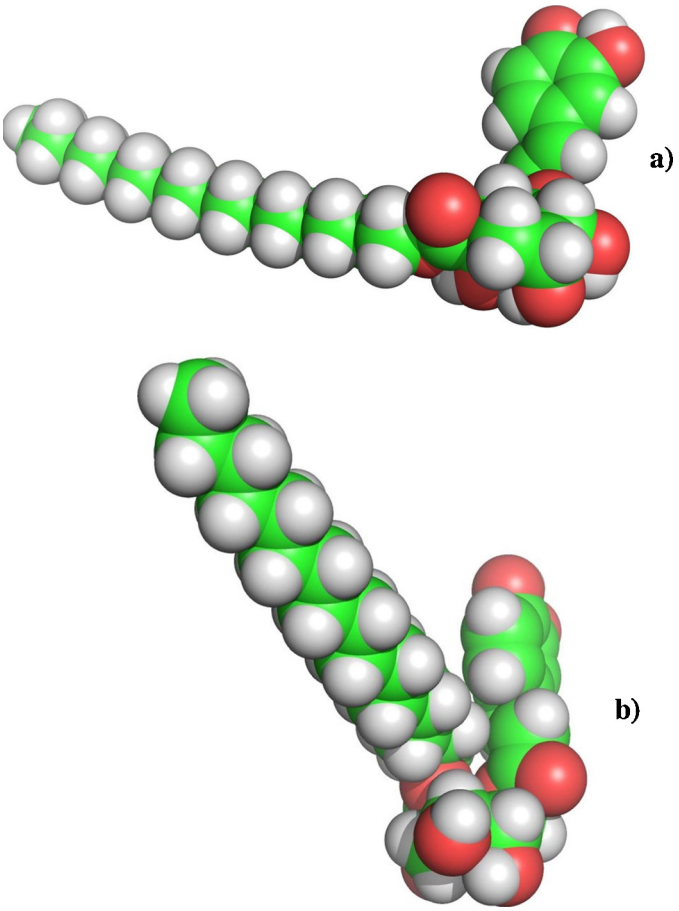

Fig. 7. Hexadecyl chlorogenate conformations by molecular modeling. (a) $_1C^4$ conformation and (b) $_4C^1$ conformation.

4. Conclusion

In the present study, semi-crystalline powders were obtained for the amylose–hexadecyl chlorogenate and amylose–3-*O*-palmitoyl chlorogenic acid assemblies and the corresponding calorimetry and solid state NMR signatures were observed and compared to the reference (amylose without ligand).

The results from differential scanning calorimetry clearly indicate the presence of an amylose complex for the amylose–3-*O*-palmitoyl chlorogenic acid assemblies with the well-known melting/recrystallization reversibility of amylose–ligand complexes. The low melting temperature observed (around 80 °C) could be interpreted by the poor crystallinity of the complexes. In contrast, the thermogram of amylose–hexadecyl chlorogenate assemblies was very similar to the reference, thereby showing no complexation of hexadecyl chlorogenate with amylose. DSC study has shown to be an efficient technique to highlight the complexes presence.

The ^{13}C CP/MAS NMR signatures obtained for the both assemblies permit to confirm the DSC results and show also that 3-*O*-palmitoyl chlorogenic acid forms complexes with the V_{6I} form. It can be concluded that only the graft is included in the helical cavity of amylose.

It was shown that the grafting of an aliphatic chain on chlorogenic acid was required for observing the complexation of the amylose (Lorentz et al., 2012). This work clearly showed that the position of the graft has strong consequences on the complexing of amylose. A molecular modeling study has been performed on the molecules and its graft position to assess if the conformation of the derivative grafted could explain the experimental results.

Results showed that molecular modeling explains the difference in behavior of the three chlorogenic acid derivatives relative to amylose. The tilting of the quinic ring into the $_4C^1$ form causes a steric hindrance making it improbable for amylose to form a complex with the aliphatic chain grafted on the C1. Moreover, the $_4C^1$ form does not involve any difficulty for the complexation of the C16 chain in the C3 or C4 position. These results show the importance of the grafting position on the ring of quinic acid.

Acknowledgement

This work was financed in part by the regional program: Integrated Approach of Food Safety and Food Quality (Pays de la Loire region, France).

References

Biais, B., Le Bail, P., Robert, P., Pontoire, B., & Buleon, A. (2006). Structural and stoichiometric studies of complexes between aroma compounds and amylose. Polymorphic transitions and quantification in amorphous and crystalline areas. *Carbohydrate Polymers*, *66*, 306–315.

Biliaderis, C. G., & Galloway, G. (1989). Crystallization behavior of amylose–V complexes: Structure–property relationships. *Carbohydrate Research*, *189*, 31–48.

Biliaderis, C. G., Page, C. M., Slade, L., & Sirett, R. R. (1985). Thermal behavior of amylose–lipid complexes. *Carbohydrate Polymers*, *5*, 367–389.

Brisson, J., Chanzy, H., & Winter, W. T. (1991). The crystal and molecular structure of Vh amylose by electron diffraction analysis. *International Journal of Biological Macromolecules*, *13*(2), 31–39.

Buléon, A., Delage, M. M., Brisson, J., & Chanzy, H. (1990). Single crystals of V amylose complexed with isopropanol and acetone. *International Journal of Biological Macromolecules*, *12*(2), 25–33.

Chebil, L., Humeau, C., Falcimaigne, A., Engasser, J., & Ghoul, M. (2006). Enzymatic acylation of flavonoïds. *Process Biochemistry*, *11*(41), 2237–2251.

Clifford, M. (1999). Chlorogenic acids and other cinnamates-nature, occurrence and dietary burden, adsorption and metabolism. *Journal of Science of Food and Agriculture*, *79*, 362–372.

Figueroa-Espinoza, M. C., & Villeneuve, P. (2005). Phenolic acids enzymatic lipophilization. *Journal of Agricultural and Food Chemistry*, *8*(53), 2779–2787.

Gidley, M. J., & Bociek, S. M. (1985). Molecular organization in starches: A ^{13}C CP/MAS NMR study. *Journal of the American Chemical Society*, *107*, 7040–7044.

Gidley, M. J., & Bociek, S. M. (1988). ^{13}C CP/MAS NMR Studies of amylose inclusion complexes, cyclodextrins, and the amorphous phase of starch granules: Relationships between glycosidic linkage conformation and solid state ^{13}C chemical shifts. *Journal of the American Chemical Society*, *110*, 3820–3829.

Godet, M. C., Bizot, H., & Buléon, A. (1995). Crystallization of amylose–fatty acid complexes prepared with different amylose chain lengths. *Carbohydrate Polymers*, *27*, 47–52.

Godet, M. C., Buléon, A., Tran, V., & Colonna, P. (1993). Structural features of fatty acid–amylose complexes. *Carbohydrate Polymers*, *21*, 91–95.

Godet, M. C., Tran, V., Colonna, P., Buléon, A., & Pezolet, M. (1995). Inclusion/exclusion of fatty acids in amylose complexes as a function of the fatty acid chain length. *International Journal of Biological Macromolecules*, *17*(6), 405–408.

Horii, F., Yamamoto, H., Hirai, A., & Kitamaru, R. (1987). Structural study of amylose polymorphs by cross-polarization-magic angle spinning, ^{13}C-NMR spectrometry. *Carbohydrate Polymers*, *160*, 29–40.

Ingraham, J., & Corse, J. (1951). Enzymatic browning of fruits. I. Autoxidation of chlorogenic acid. *Journal of the American Chemical Society*, *73*, 5550–5553.

Kono, Y., Kobayashi, K., Tagawa, S., Adachi, K., Ueda, A., & Sawa, Y. (1997). Antioxidant activity of polyphenolics in diets: Rate constants of reactions of chlorogenic acid and caffeic acid with reactive species of oxygen and nitrogen. *Biochemica Biophysica Acta*, *1335*, 335–342.

Le Bail, P., Rondeau, C., & Buléon, A. (2005). Structural investigation of amylose complexes with small ligands: Helical conformation, crystalline structure and thermostability. *International Journal of Biological Macromolecules*, *35*, 1–7.

Lorentz, C., Dulac, A., Pencreac'h, G., Ergan, F., Richomme, P., & Soultani, S. (2010). Lipase-catalysed synthesis of 4-0- and 3-0-palmitoyl chlorogenic acids as new antioxidants. *Biotechnology Letters*, *32*, 1955–1960.

Lorentz, C., Pencreac'h, G., Soultani-Vigneron, S., Rondeau-Mouro, C., de Carvalho, M., Pontoire, B., et al. (2012). Coupling lipophilization and amylose complexation to encapsulate chlorogenic acid. *Carbohydrate Polymers*, *90*(1), 152–158.

Martin, R., Lilley, T. H., Fasshaw, C. P., Begley, M. J., & Magnolato, D. (1987). The caffeine–potassium chlorogenate molecular complex. *Phytochemistry*, *26*(1), 273–279.

Nuessli, J., Sigg, B., Conde-Petit, B., & Escher, F. (1997). Characterization of amylose–flavour complexes by DSC and X-ray diffraction. *Food Hydrocolloids*, *11*(1), 27–34.

Paris, M., Bizot, H., Emery, J., Buzaré, J. Y., & Buleon, A. (1999). Crystallinity and structuring role of water in native and recrystallized starches by ^{13}C CP/MAS NMR spectroscopy. 1: Spectral decomposition. *Carbohydrate Polymers*, *39*, 327–339.

Paris, M., Bizot, H., Emery, J., Buzaré, J. Y., & Buléon, A. (2001). NMR local range investigations in amorphous starchy substrates I. Structural heterogeneity probed by ^{13}C CP-MAS NMR. *International Journal of Biological Macromolecules*, *29*, 127–136.

Rappenecker, G., & Zugenmaier, P. (1981). Detailed refinement of the crystal structure of Vh–amylose. *Carbohydrate Research*, *89*, 11–19.

Shi, G., Rao, L., Yu, H., Xiang, H., Pen, G., Long, S., et al. (2007). Yeast-cell-based microencapsulation of chlorogenic acid as a water-soluble antioxidant. *Journal of Food Engineering*, *80*, 1060–1067.

Singh, V., Ali, S. I., & Divakar, S. (1993). ^{13}C CP/MAS NMR spectroscopy of native and acid modified starches. *Starch*, *45*, 59–62.

Sun-Waterhouse, D. (2011). The development of fruit-based functional foods targeting the health and wellness market: A review. *International Journal of Food Science and Technology*, *46*(5), 899–920.

Veregin, R. P., Fyfe, C. A., Marchessault, R. H., & Taylor, A. J. (1986). Characterization of the crystalline A and B starch polymorphs and investigation of starch crystallization by high resolution ^{13}C CP/MAS NMR. *Macromolecules*, *19*, 1030–1034.

Veregin, R. P., Fyfe, C. A., Marchessault, R. H., & Taylor, A. J. (1987). Correlation of ^{13}C chemical shifts with torsional angles from high-resolution, ^{13}C-CP-MAS NMR studies of crystalline cyclomalto–oligosaccharide complexes, and their relation to the structures of the starch polymorphs. *Carbohydrate Research*, *160*, 41–56.

Veregin, R. P., Fyfe, C. A., Marchessault, R. H., & Taylor, M. G. (1987). Investigation of the crystalline V amylose complexes by high-resolution carbon-13 CP/MAS NMR spectroscopy. *Macromolecules*, *20*, 3007–3012.

Villeneuve, P. (2007). Lipases in lipophilization reactions. *Biotechnology Advances*, *6*(25), 515–536.

Zang, L., Cosma, G., Gardner, H., Castranova, V., & Vallyathan, V. (2003). Effect of chlorogenic acid on hydroxyl radical. *Molecular and cellular biochemistry*, *247*, 205–210.

Zhao, M., Wang, H., Yang, B., & Tao, H. (2010). Identification of cyclodextrin inclusion complex of chlorogenic acid and antimicrobial activity. *Food Chemistry*, *120*, 1138–1142.